

Body mass trajectories and cortical thickness in middle-aged men: a 42-year longitudinal study starting in young adulthood



Carol E. Franz^{a,*}, Hong Xian^b, Daphne Lew^b, Sean N. Hatton^a, Olivia Puckett^a, Nathan Whitsel^a, Asad Beck^c, Anders M. Dale^d, Bin Fang^a, Christine Fennema-Notestine^{a,d}, Richard L. Hauger^{a,e}, Kristen C. Jacobson^f, Michael J. Lyons^g, Chandra A. Reynolds^h, William S. Kremen^{a,e}

^a Department of Psychiatry & Center for Behavior Genetics of Aging, University of California San Diego, La Jolla, CA, USA

^b Department of Epidemiology & Biostatistics, St. Louis University, St. Louis, MO, USA

^c Department of Psychology, San Diego State University, San Diego, CA, USA

^d Department of Radiology, University of California San Diego, La Jolla, CA, USA

^e Center of Excellence for Stress and Mental Health, VA San Diego Healthcare System, USA

^f Department of Psychiatry & Behavioral Neuroscience, University of Chicago, Chicago, IL, USA

^g Department of Psychological and Brain Sciences, Boston University, Boston, MA, USA

^h Department of Psychology, University of California Riverside, Riverside, CA, USA

ARTICLE INFO

Article history:

Received 16 August 2018

Received in revised form 1 March 2019

Accepted 5 March 2019

Available online 12 March 2019

Keywords:

Obesity

Body mass index (BMI)

Trajectory

Longitudinal

Cortical thickness

White matter abnormalities

ABSTRACT

Evidence strongly suggests that being overweight or obese at midlife confers significantly higher risk for Alzheimer's disease and greater brain atrophy later in life. Few studies, however, examine associations between longitudinal changes in adiposity during early adulthood and later brain morphometry. Measures of body mass index (BMI) were collected in 373 men from the Vietnam Era Twin Study of Aging at average ages 20, 40, 56, and 62 years, yielding 2 BMI trajectories. We then examined associations between BMI phenotypes (trajectories, continuous BMI, obese/nonobese), cortical thickness, and white matter measures from structural magnetic resonance imaging at mean age 62 (time 4, range 56–66 years). Those on the obesity trajectory ($N = 171$) had a thinner cortex compared with the normal/lean trajectory ($N = 202$) in multiple frontal and temporal lobe bilateral regions of interest: superior, inferior, middle temporal gyri, temporal pole, fusiform gyrus, banks of the superior temporal sulcus, frontal pole, pars triangularis, caudal and rostral middle frontal gyri (all $p < 0.05$, false discovery rate corrected). Frontal lobe thinness tended to occur mainly in the right hemisphere. Results were similar for obese versus nonobese adults at age 62. There were no significant differences for white matter volume or abnormalities. Taken in the context of other research, these associations between brain structures and excess BMI at midlife suggest potential for increased risk for cognitive decline in later life.

© 2019 Elsevier Inc. All rights reserved.

1. Introduction

Obesity has long been established as a leading cause of morbidity and mortality among adults in the United States (U.S.), with significantly worse cardiometabolic outcomes emerging as early as midlife (Grundy, 2004; Reilly and Kelly, 2011; Reis et al., 2015; Twig et al., 2016; Xian et al., 2017). Evidence strongly suggests that being overweight or obese at midlife also confers significantly higher risk

for Alzheimer's disease (AD) and greater brain atrophy later in life (Albanese et al., 2017; Santos et al., 2017a, b; Shaw et al., 2017, 2018; Singh-Manoux et al., 2018). (Chuang et al., 2016), for example, reported that each unit increase in body mass index (BMI) at midlife was associated with a 1%–2% average brain tissue reduction in the frontal, temporal, and occipital lobes in late life, as well as with earlier onset of AD, greater Braak neurofibrillary tangle scores, and greater amyloid burden.

A major review of 44 studies concluded that greater adiposity (most frequently measured as BMI) is associated with smaller total gray matter (GM) volume; no consistent evidence was found, however, for adiposity effects on white matter (WM) volume or abnormalities (Willette and Kapogiannis, 2015). Findings varied by

* Corresponding author at: Department of Psychiatry, University of California San Diego, 9500 Gilman Dr, MC 0738, La Jolla, CA 92093, USA. Tel.: +1 858 822-1793; fax: +1 858 822-5856.

E-mail address: cfranz@ucsd.edu (C.E. Franz).

age (<40 vs. 40+), gender, and measurement approach. The strongest results were for measures of categorical obesity rather than continuous BMI and for prefrontal, frontal, temporal, and posterior cingulate regions. Many studies did not adjust for cardiovascular/cardiometabolic factors (Coutinho et al., 2017; Krishnadas et al., 2013; Walhovd et al., 2014). Most studies reviewed were cross-sectional, relatively small, focused on older adults, and examined global measures and cortical volumes. Thus, increased focus on specific brain regions and on younger adults is warranted.

Literature has emerged showing that it is also important to examine thickness or surface area separately rather than simply focusing on cortical volume (Panizzon et al., 2009; Vuoksimaa et al., 2015). For instance, having a thinner cortex as adulthood progresses is thought to be related to degenerative processes due to key features such as organization of cortical layers, cell bodies in neurons, and synaptic connections, as well as cortical vulnerability to environmental influences (Fjell et al., 2014). (Shaw et al., 2017) reported that increasing BMI over 8 years in 404 adults aged 44–49 years predicted thinning in the posterior and caudal anterior cingulate, lingual gyrus, and pericalcarine regions of the cortex. In a 2-group study comparing the above 44- to 49-year-old (midlife) adults with a group of 60- to 66-year-old (late-life) adults, baseline BMI was associated with cortical thickness in late life but not in midlife—most notably in the bilateral entorhinal cortex and bilateral cingulate (Shaw et al., 2018). Increasing BMI across 8 years was associated with cortical thinning in 6 lateral regions of interest (ROIs) in the late-life group and 1 ROI in the midlife group. (Medic et al., 2016) found that among adults aged 18–50 years, 2 cortical regions (ventromedial prefrontal cortex and lateral occipital cortex) were significantly thinner in obese participants. Together, these findings suggest that BMI-related brain differences typically found in older adults may already be present by midlife.

In the present study, we examined relationships between BMI assessed 4 times across 4 decades starting at mean age 20 and cortical thickness, WM volume, and WM abnormalities in late midlife (approximately age 62). We predicted that adults on an obesity trajectory (where BMI rapidly increases toward obese levels) would be more likely than adults on a normal/lean BMI trajectory (where BMI stays relatively flat and close to normal levels) to have thinner cortices in frontal and temporal regions in late midlife. Analyses examined both bilateral and hemisphere-specific associations. To further elucidate these associations, we also conducted analyses with other BMI phenotypes: BMI measured continuously and obese versus nonobese groups (BMI \geq 30; BMI < 30). Next, we qualitatively visualized regions affected by BMI trajectories using exploratory vertexwise cortical thickness analysis. Finally, we rigorously examined associations of BMI with WM volume and WM abnormalities. Along with the use of longitudinal BMI data, the inclusion of many factors such as hypertension, fasting glucose, triglyceride, cholesterol, and C-reactive protein is a strength of the study.

2. Material and methods

2.1. Participants

Participants were from the Vietnam Era Twin Study of Aging (VETSA) (Kremen et al., 2013b), a longitudinal study of risk and protective factors for cognitive and brain aging in a community-dwelling sample of men from across the U.S. VETSA participants were recruited as a simple random sample from the all-male Vietnam Era Twin Registry (Goldberg et al., 2002), a research registry of twins who all served in the U.S. military sometime between 1965 and 1975. VETSA 1 (2002–2008) eligibility included being 51–59 years old when recruited and both members of a twin pair

agreed to participate (Kremen et al., 2006). The VETSA 2 (2009–2013) follow-up occurred approximately 6 years later (Kremen et al., 2013a, b). VETSA participants comprise a representative epidemiological sample of community-based men with regard to marital, work, income, and health characteristics of American men in their age range based on U.S. Census and Center for Disease Control data (Schoenborn and Heyman, 2009). As a sample of veterans, at baseline, VETSA participants constitute a group with no major chronic childhood health problems. The military recruitment standards mandate weight-for-height and maximum body fat limits (with occasional waivers for underweight or overweight recruits); thus, the majority of the participants were not obese at baseline (98%) (Cawley and Maclean, 2012). Nearly 80% of VETSA participants report no combat experience. More details about the VETSA magnetic resonance imaging (MRI) sample and data collection are published elsewhere (Fennema-Notestine et al., 2016; Kremen et al., 2013a).

2.2. Procedures

This study utilizes BMI data collected from the same participants at 4 timepoints: baseline (time 1; mean age 19.9 years, SD = 1.4; range 18–24); a 1990 National Heart, Lung, and Blood Institute survey (time 2; mean age 40.3 years, SD = 2.7; range 35–44) (Goldberg et al., 2002), and in-person evaluations at either the University of California San Diego (UCSD) or Boston University (BU) at VETSA 1 (time 3; mean age 56.3 years, SD = 2.6; range 51–60) and VETSA 2 (time 4; mean age 61.9 years, SD = 2.6; range 56–66). On the day following the time 4 in-person assessment, the subsample of MRI eligible participants (N = 426) underwent structural MRI at either the UCSD or Massachusetts General Hospital (MGH).

Institutional review board approval was obtained at all sites, and participants provided written informed consent.

2.3. Measures

2.3.1. BMI

Height and weight were objectively measured at times 1, 3, and 4 as part of physical examinations. Time 1 occurred at the military induction physical. Time 2 height and weight were self-reported as part of a mailed survey. Self-reported height and weight are considered valid measures but can be biased depending on age, gender, and ethnicity (Connor-Gorber et al., 2007; Richmond et al., 2015). At times 3 and 4, participants were weighed in-person on a digital scale after removing shoes, heavy outer clothing, and pocket items. Height was assessed, in stocking feet, with a stadiometer. After transforming height and weight to metric units, BMI was calculated as kg/m². As reported earlier, height was highly correlated across times 2, 3, and 4 when full adult height had been reached (Xian et al., 2017).

BMI trajectories were derived previously (Xian et al., 2017) using continuous measures of BMI and latent class growth modeling in Mplus, version 7.4 (Muthen and Muthen, 2015). In latent class growth modeling, each participant receives a membership probability for each mutually exclusive trajectory based on the BMI change pattern over time and is assigned to the trajectory with the highest probability. Although 3 BMI trajectories across the 4 timepoints were identified in the full sample (Xian et al., 2017), 1 group contained only 13 participants in the MRI subsample. For these analyses, we combined the 2 trajectories with rapidly increasing BMI; because both ended in obesity, we call this combined trajectory the obesity trajectory (N = 171). The group that maintained BMI with a relatively flat slope remaining close to the normal BMI range across the 4 decades we called the normal BMI trajectory (N = 202; see Table 1 for descriptive information). BMI was the only

Table 1
Demographics by BMI trajectory

Variables (mean/SD)	Normal trajectory, N = 202, mean (SD)	Obese trajectory, N = 171, mean (SD)	p-value
Age at MRI (time 4)	62.0 (2.48)	61.7 (2.65)	<i>p</i> = 0.20
Education (y)	14.0 (2.09)	13.7 (1.96)	<i>p</i> = 0.24
AFQT time 1	0.39 (0.67)	0.41 (0.68)	<i>p</i> = 0.72
Ethnicity (% WNH)	90.8%	83.1%	<i>p</i> = 0.03
BMI time 1/age 20, kg/m ²	21.4 (2.22)	23.7 (2.80)	<i>p</i> < 0.0001
% obese	0%	3.5%	
BMI time 2/age 40, kg/m ²	23.6 (1.90)	27.4 (3.01)	<i>p</i> < 0.0001
% obese	0%	10.5%	
BMI time 3/age 56, kg/m ²	25.7 (2.41)	31.7 (2.92)	<i>p</i> < 0.0001
% obese	2.9%	69.9%	
BMI time 4/age 62, kg/m ²	25.9 (2.48)	32.6 (3.00)	<i>p</i> < 0.0001
% obese	2.5%	82%	
Time 4/age 62 cardiometabolic risk factors			
C-reactive protein risk	18.7%	34.9%	<i>p</i> = 0.01
Hypertension risk	59.7%	85%	<i>p</i> < 0.0001
Diabetes risk	41.4%	58%	<i>p</i> = 0.01
Hypercholesterolemia risk	58.5%	70.1%	<i>p</i> = 0.03
Ischemic heart disease risk	10.2%	11.7%	<i>p</i> = 0.66
Metabolic syndrome risk	17.4%	59.4%	<i>p</i> < 0.0001
Smoking			
% Never	86 (42.6)	66 (38.6)	<i>p</i> = 0.29
% Former	74 (36.6)	76 (44.4)	
% Current	42 (20.8)	29 (17.0)	

Key: SD, standard deviation; BMI, body mass index; WNH, white non-hispanic; AFQT, armed forces qualification test (Uhlener JE, Bolanovich DJ. *Development of the Armed Forces Qualification Test and Predecessor Army Screening Tests, 1946–1950*. Washington, DC: Personnel Research Section, Department of the Army, 1952.).

indicator of adiposity available at all 4 timepoints. Separate measures of obese/not obese (BMI ≥ 30 /BMI < 30, respectively) were created at each timepoint.

2.3.2. MRI acquisition and processing

2.3.2.1. Cortical thickness and white matter volume. At time 4, T1-weighted images were acquired on a GE 3T Discovery 750 scanner (GE Healthcare, Waukesha, WI, USA) with an 8-channel phased array head coil at the UCSD and a Siemens Tim Trio (Siemens USA, Washington, D.C., USA) with a 32-channel head coil at MGH. At the UCSD, the 3D fast spoiled gradient echo (FSPGR) T1-weighted image protocol was as follows: echo time (TE) = 3.164 ms, repetition time (TR) = 8.084 ms, time to inversion (TI) = 600 ms, flip angle = 8°, pixel bandwidth = 244.141, field of view (FOV) = 24 cm, frequency = 256, phase = 192, slices = 172, slice thickness = 1.2 mm. At MGH, the 3D magnetization-prepared rapid gradient echo (MPRAGE) T1-weighted image protocol was as follows: TE = 4.33 ms, TR = 2170 ms, TI = 1100 ms, flip angle = 7°, pixel bandwidth = 140, slices = 160, slice thickness = 1.2 mm.

Raw image files were processed using an automated stream developed by the UCSD Center for Multimodal Imaging and Genetics under the direction of Dr. Dale. Images were corrected for gradient distortions (Jovicich et al., 2006) and B1 field inhomogeneity (Sled et al., 1998). Any images with severe scanner artifacts or excessive head motion were excluded (see section 2.3.2.3). T1-weighted images were then processed via the FreeSurfer v5.1 pipeline (Fischl, 2012) for WM volume and for cortical parcellation data derived from the Desikan-Killiany Atlas (Desikan et al., 2006). All processed images were visually reviewed for quality, and the cortical surface-related images were edited for technical accuracy in alignment with standard, objective rules to improve the brain mask (removing nonbrain voxels) and WM volume (filling hyperintense WM lesions).

2.3.2.2. White matter abnormalities. Measured WM abnormalities may include WM hyperintensities of presumed vascular origin, lacunes, and small subcortical infarcts (all hyperintense on T2-weighted or FLAIR and isointense or hypointense regions on T1) (Fennema-Notestine et al., 2016). To examine WM lesion load, T2-

and proton-density (PD)-weighted images also were acquired in the same session. At the UCSD, the T2-weighted coronal 2D fast recovery fast spin echo (FRFSE-XL) protocol was as follows: TE = 94 ms, TR = 4.6 seconds, flip angle = 90°, pixel bandwidth = 122, FOV = 24 cm, frequency = 256, phase = 256, slices = 96, slice thickness = 2 mm, echo trail length (ETL) = 16, number of excitations (NEX) = 2. The PD-weighted coronal 2D FSE-XL protocol was as follows: TE = 13 ms, TR = 3 seconds, flip angle = 90°, pixel bandwidth = 122, FOV = 24 cm, frequency = 256, phase = 256, slices = 96, slice thickness = 2 mm, ETL = 4, NEX = 1. At MGH, the T2-weighted coronal 2D turbo spin echo protocol was as follows: TE = 93 ms, TR = 4.7 seconds, flip angle = 116°, pixel bandwidth = 219, FOV = 24 cm, frequency = 123, phase = 92, slices = 96, slice thickness = 2 mm, ETL = 24, NEX = 2. The PD-weighted coronal 2D turbo spin echo protocol was as follows: TE = 19 ms, TR = 3 seconds, flip angle = 116°, pixel bandwidth = 219, FOV = 24 cm, frequency = 23, phase = 192, slices = 96, slice thickness = 2 mm, ETL = 12, NEX = 2.

White matter abnormality volume was determined using a multichannel (T1-, T2-, and PD-weighted) segmentation approach (Fennema-Notestine et al., 2016). The T1 image was rigidly aligned to standard space, and then the T2 and PD images were registered to the T1 and nonparametric nonuniform intensity normalization (N3) bias-corrected (Sled et al., 1998). A 3-class tissue segmentation calculated the robust means and covariances for WM, GM, and CSF. Abnormal voxel clusters were identified as voxels originally segmented as GM that was situated within anatomically defined WM regions. All results were visually reviewed, and misclassifications were manually corrected. Volumes were measured in each participant's native (undeformed) space. To avoid misclassification due to partial voluming errors, any voxels that touched (i.e., shared a common face, edge, or vertex with) a ventricular fluid voxel were excluded from all analyses.

2.3.2.3. MRI scan exclusion criteria. Initially, there were a total of 416 cases available that acquired all 3 scans (T1, T2, and PD). From this, 4.3% (n = 18) were excluded for motion artifact degrading quality in 1 or more of the 3 scans and 25 additional cases (4.7% at BU and 5.4% at UCSD) were excluded due to poor image processing

information (including 3 with medical conditions that made for poor segmentation) that could not be resolved by standard manual intervention. The proportion did not differ by site for either reason. A final total of 373 participants with complete MRI data remained in the analytic sample.

2.3.3. Covariates

Covariates included in analyses were age, lifetime education, ethnicity, smoking status, and being at risk for hypertension, dyslipidemia, diabetes, inflammation, and/or ischemic heart disease at time 4. Blood pressure was based on the average of 4 systolic and diastolic blood pressure (SBP and DBP) readings taken during the assessment day. Individuals with either SBP > 140 or DBP > 90 mm Hg (Aronow et al., 2011) or who took antihypertensive medication were classified as at risk for hypertension (75.1%). Fasting plasma glucose was assayed with spectrophotometry as part of a comprehensive metabolic panel; glucose levels > 5.54 mmol/L (comparable to 100 mg/dL) were considered at risk. Being at risk for diabetes was defined as having at-risk levels of glucose and/or taking a prescription medication for diabetes (51.7%) as per the International Diabetes Federation global consensus: (http://www.idf.org/webdata/docs/IDF_Meta_def_final.pdf). Triglycerides and high-density lipoprotein (HDL) cholesterol were assayed as part of a lipid panel via spectrophotometry. At-risk HDL-cholesterol was defined as levels <1.03 mmol/L (28.9%); at-risk triglycerides was classified as >1.68 mmol/L (31.5%). At-risk overall cholesterol was defined as being at risk for either HDL or triglycerides or taking cholesterol-lowering medication (72% at-risk) (Grundy, 2004). High-sensitivity C-reactive protein (CRP), a protein measured in blood that indicates inflammation, was assayed using nephelometry (Mora et al., 2009), and at-risk inflammation was defined as CRP > 28.5 nmol/L (27.5%). Presence/absence of ischemic heart disease at time 4 (18%) was coded using a validated population-based index (Xian et al., 2010), indicating presence of angina based on a positive Rose Angina score and/or a prescription for nitroglycerin (Lampe et al., 1999), self-reported heart attack/myocardial infarction, and/or heart surgery. Ethnicity was coded as white non-Hispanic versus other. Tobacco smoking was coded as never, former, or current. Lifetime education reflected the number of years of formal schooling completed (e.g., secondary school diploma = 12; 4-year college degree = 16; PhD/MD = 20).

2.4. Data analyses

2.4.1. Linear mixed model analyses

Left and right hemisphere ROI measures were averaged to obtain bilateral ROI measures. Because different scanners were used at the 2 sites, all MRI measures adjusted for scanner. Cortical thickness measures also adjusted for weighted mean cortical thickness, calculated as the sum of all cortical volume ROIs divided by the total surface area. These ROIs were then used in the linear mixed model statistical analyses. White matter measures were adjusted for intracranial volume to account for individual differences in head size. Analyses included the random effect of family to account for the twin clustering of the data and covariates described in Section 2.3.3.

Linear mixed models were used to examine associations between neuroimaging measures and BMI phenotypes. Statistical analyses used Proc Mixed in SAS, version 9.4 (SAS Institute, Cary, NC, USA). We followed up the BMI trajectory comparisons of ROIs with vertexwise analyses and hemisphere-based analyses, including the same covariates. Finally, we examined associations between obese/nonobese groups and continuous BMI with the cortical thickness continuous measures at time 4. All *p*-values are 2-tailed. Results reflect false discovery rate (FDR) corrections at *p* <

0.05 (2-tailed) for multiple comparisons (Benjamini and Hochberg, 1995; Li and Ji, 2005).

2.4.2. Vertexwise analyses

We conducted an exploratory vertexwise analysis to qualitatively examine regions of the cortex that could be affected by BMI, by hemisphere. This offered a visual perspective of the regions affected but is limited by the constraints of the generalized linear model that does not permit the inclusion of missing data or random effects (i.e., twin relatedness), which linear mixed models can incorporate.

Cortical vertexwise analysis was conducted in Matlab r2014a using the Matlab FreeSurfer and Statistical toolboxes. Cortical thickness maps for each hemisphere were concatenated and a general linear mixed model was run contrasting the BMI trajectories (different intercept, different slope) while controlling for education, ethnicity, age, and being at risk for dyslipidemia, hypertension, diabetes, or ischemic heart disease, and scanner. To improve sensitivity and signal to noise ratio, we applied a 30-mm full-wide half-maximum smoothing kernel recommended for cortical thickness (Lerch and Evans, 2005). It should be noted that this smoothing does inherently reduce specificity and anatomical precision (Bernal-Rusiel et al., 2010). Significance was set at *p* < 0.05 (FDR-corrected) for clusters larger than 100 voxels, and statistical maps were rendered over the FreeSurfer average brain.

3. Results

3.1. Descriptive results

Comparisons between normal BMI and obesity trajectories revealed no differences in cognitive ability at time 1 (average age 20), education, or age (Table 1). The normal BMI trajectory (*N* = 202) was significantly more likely to be white non-Hispanic (91%) compared with the obesity trajectory (83%). Mean BMI in the obesity trajectory (*N* = 171) was significantly higher at all 4 time-points. As shown in Table 1, compared with the normal BMI trajectory, members of the obesity trajectory were more likely to have at-risk levels of CRP, diabetes, SBP, and DBP at time 4 (average age 62). Risk for metabolic syndrome—that is, the co-occurrence of 3 or more cardiometabolic risk indicators (i.e., at risk for obesity, dyslipidemia, hypertension, diabetes)—occurred more frequently in the obesity trajectory (59.4%) compared with the normal BMI trajectory (17.4%). Rates of ischemic heart disease or smoking were not significant.

3.2. BMI trajectories and bilateral ROI cortical thickness

The obesity trajectory compared with the normal BMI trajectory had significantly thinner cortex in multiple bilateral frontal ROIs (i.e., frontal pole, pars triangularis, and caudal and rostral middle frontal gyri ROIs) and temporal lobe (i.e., banks of the superior temporal sulcus; inferior, middle, and superior temporal gyri; fusiform gyrus; temporal pole) (Table 2, Fig. 1). No regions in the cingulate, occipital lobe, or parietal lobe were different after FDR correction.

3.3. Obese/nonobese group comparisons, continuous BMI, and bilateral ROI cortical thickness

We examined the extent to which categorical BMI (obese/not obese) or continuous BMI at each timepoint, adjusted for all covariates, were associated with cortical thickness at time 4. Obesity at time 1 or 3 (average age 56) did not predict any midlife brain outcome. At time 2 (average age 40), 1 comparison survived FDR

Table 2

Comparisons of cortical thickness regions of interest at time 4 (~ age 62) in normal versus obese BMI trajectory groups

Time 4/age 62 MRI regions of interest		Left hemisphere		Right hemisphere		Bilateral	
		Point estimate (95% CI)	p-value	Point estimate (95% CI)	p-value	Point estimate (95% CI)	p-value
Cingulate							
	Isthmus of cingulate gyrus	−0.0280 (−0.0762, 0.0193)	0.2405	−0.0097 (−0.0570, 0.0377)	0.6864	−0.0141 (−0.0558, 0.0276)	0.5039
	Caudal anterior cingulate	−0.0104 (−0.0741, 0.0533)	0.7475	−0.0340 (−0.0938, 0.0258)	0.2615	−0.0225 (−0.0725, 0.0276)	0.3748
	Rostral posterior cingulate	−0.0304 (−0.0679, 0.0071)	0.1112	−0.0249 (−0.0646, 0.0149)	0.2171	−0.0268 (−0.0594, 0.0058)	0.1066
	Rostral anterior cingulate	−0.0658 (−0.1210, −0.0105)	0.0201	−0.0399 (−0.0930, 0.0132)	0.1389	−0.0506 (−0.0952, −0.0059)	0.0267
Frontal lobe							
	Frontal pole	−0.0612 (−0.1264, 0.0039)	0.0650	−0.0621 (−0.1275, 0.0033)	0.0627	−0.0675 (−0.1211, −0.0140)	0.0149^a
	Paracentral lobule	0.0072 (−0.0299, 0.0443)	0.7000	−0.0105 (−0.0490, 0.0279)	0.5878	0.0020 (−0.0318, 0.0359)	0.9052
	Precentral gyrus	−0.0313 (−0.0701, 0.0076)	0.1133	−0.0531 (−0.0903, −0.0160)	0.0055^a	−0.0424 (−0.0779, −0.0069)	0.0199
	Superior frontal gyrus	−0.0142 (−0.0473, 0.0188)	0.3943	−0.0296 (−0.0604, 0.0012)	0.0598	−0.0201 (−0.0506, 0.0103)	0.1927
	Pars opercularis	−0.0132 (−0.0497, 0.0233)	0.4755	−0.0556 (−0.0948, −0.0163)	0.0060	−0.0343 (−0.0670, −0.0016)	0.0397
	Pars orbitalis	−0.0530 (−0.1054, −0.0006)	0.0473	0.0099 (−0.0379, 0.0577)	0.6819	−0.0234 (−0.0650, 0.0182)	0.2677
	Pars triangularis	−0.0317 (−0.0735, 0.0102)	0.1370	−0.0673 (−0.1032, −0.0313)	0.0003^a	−0.0481 (−0.0824, −0.0139)	0.0064^a
	Caudal middle frontal gyrus	−0.0274 (−0.0645, 0.0098)	0.1471	−0.0692 (−0.1083, −0.0301)	0.0007^a	−0.0475 (−0.0819, −0.0132)	0.0071^a
	Rostral middle frontal gyrus	−0.0362 (−0.0677, −0.0046)	0.0249	−0.0575 (−0.0853, −0.0297)	0.0001^a	−0.0464 (−0.0734, −0.0193)	0.0010^a
	Lateral orbitofrontal cortex	−0.0277 (−0.0633, 0.0079)	0.1260	−0.0310 (−0.0688, 0.0067)	0.1058	−0.0304 (−0.0632, 0.0025)	0.0699
	Medial orbitofrontal cortex	−0.0301 (−0.0694, 0.0092)	0.1314	−0.0150 (−0.0579, 0.0279)	0.4908	−0.0192 (−0.0537, 0.0153)	0.2729
Occipital lobe							
	Cuneus	0.0123 (−0.0175, 0.0422)	0.4139	−0.0064 (−0.0385, 0.0258)	0.6963	0.0029 (−0.0249, 0.0307)	0.8342
	Lateral occipital cortex	−0.0105 (−0.0421, 0.0210)	0.5088	−0.0003 (−0.0336, 0.0330)	0.9851	−0.0044 (−0.0344, 0.0256)	0.7736
	Lingual gyrus	0.0091 (−0.0201, 0.0382)	0.5398	−0.0006 (−0.0302, 0.0290)	0.9703	0.0062 (−0.0206, 0.0331)	0.6473
	Pericalcarine	0.0127 (−0.0157, 0.0411)	0.3785	−0.0027 (−0.0313, 0.0259)	0.8500	0.0038 (−0.0198, 0.0274)	0.7499
Parietal lobe							
	Inferior parietal cortex	−0.0179 (−0.0509, 0.0151)	0.2843	−0.0279 (−0.0612, 0.0054)	0.0997	−0.0216 (−0.0518, 0.0087)	0.1608
	Postcentral gyrus	−0.0217 (−0.0537, 0.0103)	0.1825	−0.0365 (−0.0659, −0.0071)	0.0154	−0.0276 (−0.0552, 0.0000)	0.0499
	Precuneus	−0.0268 (−0.0580, 0.0043)	0.0907	−0.0234 (−0.0584, 0.0116)	0.1873	−0.0243 (−0.0547, 0.0060)	0.1150
	Superior parietal cortex	0.0075 (−0.0269, 0.0420)	0.6657	−0.0023 (−0.0361, 0.0315)	0.8917	0.0070 (−0.0257, 0.0397)	0.6737
	Supramarginal gyrus	−0.0340 (−0.0696, 0.0016)	0.0607	−0.0388 (−0.0725, −0.0052)	0.0242	−0.0354 (−0.0661, −0.0048)	0.0240
Temporal lobe							
	Banks of superior temporal sulcus	−0.0739 (−0.1123, −0.0356)	0.0002^a	−0.0474 (−0.0890, −0.0059)	0.0255	−0.0623 (−0.0931, −0.0315)	0.0001^a
	Inferior temporal cortex	−0.0492 (−0.0840, −0.0144)	0.0061^a	−0.0339 (−0.0695, 0.0017)	0.0620	−0.0412 (−0.0719, −0.0105)	0.0090^a
	Middle temporal gyrus	−0.0521 (−0.0864, −0.0179)	0.0032^a	−0.0500 (−0.0841, −0.0160)	0.0044^a	−0.0503 (−0.0796, −0.0211)	0.0009^a
	Superior temporal gyrus	−0.0336 (−0.0697, 0.0024)	0.0672	−0.0556 (−0.0909, −0.0204)	0.0023^a	−0.0410 (−0.0729, −0.0090)	0.0125^a
	Transverse temporal gyrus	−0.0297 (−0.0842, 0.0249)	0.2832	−0.0407 (−0.0961, 0.0148)	0.1487	−0.0339 (−0.0817, 0.0138)	0.1616
	Entorhinal cortex	−0.0573 (−0.1387, 0.0241)	0.1656	−0.0240 (−0.1094, 0.0613)	0.5778	−0.0403 (−0.1103, 0.0298)	0.2569
	Fusiform gyrus	−0.0650 (−0.0993, −0.0306)	0.0003^a	−0.0355 (−0.0692, −0.0018)	0.0389	−0.0511 (−0.0815, −0.0207)	0.0012^a
	Parahippocampal gyrus	−0.0239 (−0.0989, 0.0511)	0.5280	−0.0502 (−0.1178, 0.0174)	0.1436	−0.0355 (−0.0996, 0.0286)	0.2747
	Temporal pole	−0.0652 (−0.1397, 0.0092)	0.0853	−0.1130 (−0.1831, −0.0430)	0.0018^a	−0.0867 (−0.1460, −0.0275)	0.0045^a

Adjusted for scanner, age, ethnicity, education, smoking, at risk for hypertension, diabetes, cholesterol, inflammation, ischemic heart disease, and the random effect of family ID. MRI measures adjusted for scanner and weighted average thickness.

Key: BMI, body mass index; CI, confidence interval; FDR, false discovery rate; MRI, magnetic resonance imaging.

^a Indicates $p < 0.05$, FDR corrected (bold values). Negative sign indicates that the region is thinner in participants who are obese (BMI ≥ 30) compared with those who are not obese (BMI < 30) at time 4 (age 62).

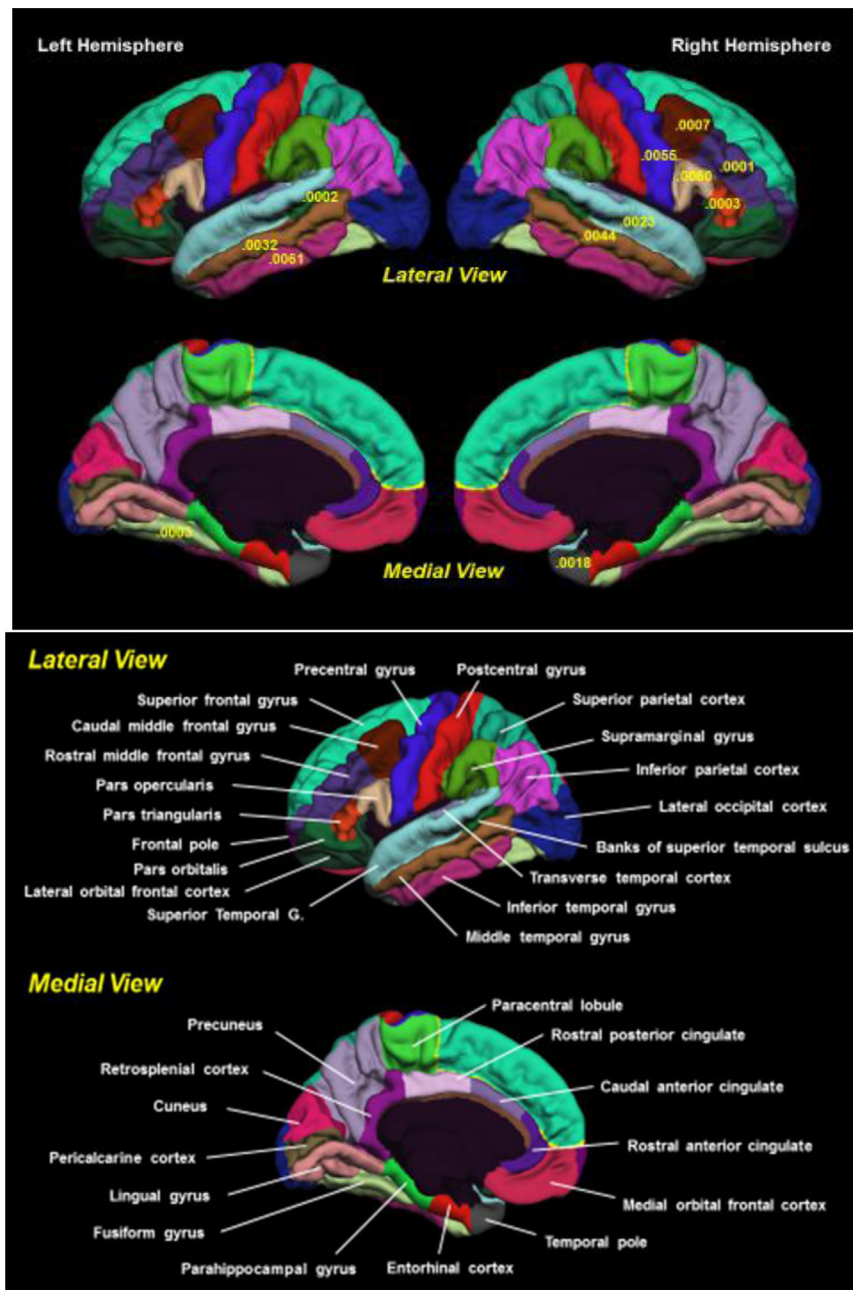


Fig. 1. Parcellation map of cortical regions associated with BMI trajectory by hemisphere (33 ROIs per hemisphere). Shown are p-values for regions that are significantly different in the obese versus the normal trajectory. All indicated ROIs are thinner for the obesity trajectory compared with the normal trajectory (see Table 2 for parameter estimates). T1-weighted images were processed via the FreeSurfer v5.1 pipeline. Cortical parcellation data were derived from the Desikan-Killiany atlas (Desikan et al., 2006). Results adjusted for age, education, ethnicity, smoking, at risk for hypertension, dyslipidemia, diabetes, inflammation, ischemic heart disease, and the random effect of family. Cortical thickness measures were adjusted for scanner and weighted average thickness. Abbreviations: BMI, body mass index; ROI, region of interest.

correction: the obese group had a significantly thicker lateral occipital gyrus than the nonobese group (Supplemental Table 1).

Within time 4, comparisons of obese versus nonobese groups closely paralleled those for the trajectory analyses, showing group differences largely in the frontal and temporal lobes (Table 3). The obese group had thinner pars triangularis, caudal and rostral middle frontal gyri, precentral gyrus, banks of the superior temporal sulcus, middle and superior temporal gyri, and fusiform gyrus compared with the nonobese group (Supplemental Fig. 1). The supramarginal gyrus of the parietal lobe was significantly thinner in the obese group. No results were significant at any time for the continuous BMI measure (data not shown).

Finally, post hoc we ran mixed effect models by hemisphere that excluded cardiometabolic risk measures (i.e., at-risk hypertension, dyslipidemia, diabetes, inflammation, ischemic heart disease) as covariates (see Supplemental Tables 2 and 3). Point estimates were largely similar, suggesting that most of the association is explained by BMI.

3.4. Lateralized cortical thickness

We first conducted an exploratory vertexwise analysis to qualitatively examine regions of the cortex that could be affected by BMI, using generalized linear models. As can be seen in Fig. 2, the

Table 3

Cross-sectional comparisons of cortical thickness regions of interest in obese versus nonobese groups at time 4 (~ age 62)

MRI measures (regions of interest)	Left hemisphere	<i>p</i> -value	Right hemisphere	<i>p</i> -value	Bilateral	<i>p</i> -value
	Point estimate (95% CI)		Point estimate (95% CI)		Point estimate (95% CI)	
Cingulate						
Isthmus of cingulate gyrus	−0.0259 (−0.0734, 0.0217)	0.2831	−0.0110 (−0.0587, 0.0366)	0.6477	−0.0155 (−0.0568, 0.0259)	0.4604
Caudal anterior cingulate	0.0191 (−0.0443, 0.0825)	0.5512	−0.0382 (−0.0984, 0.0220)	0.2108	−0.0105 (−0.0601, 0.0391)	0.6756
Rostral posterior cingulate	−0.0152 (−0.0526, 0.0222)	0.4210	−0.0070 (−0.0466, 0.0326)	0.7278	−0.0096 (−0.0417, 0.0225)	0.5543
Rostral anterior cingulate	−0.0805 (−0.1364, −0.0246)	0.0052	−0.0229 (−0.0770, 0.0311)	0.4020	−0.0491 (−0.0941, −0.0041)	0.0330
Frontal lobe						
Frontal pole	−0.0703 (−0.1362, −0.0045)	0.0366	−0.0520 (−0.1176, 0.0136)	0.1190	−0.0646 (−0.1181, −0.0112)	0.0183
Paracentral lobule	−0.0162 (−0.0528, 0.0205)	0.3833	−0.0342 (−0.0720, 0.0036)	0.0756	−0.0227 (−0.0559, 0.0104)	0.1761
Precentral gyrus	−0.0397 (−0.0791, −0.0004)	0.0480	−0.0607 (−0.0980, −0.0234)	0.0017^a	−0.0502 (−0.0859, −0.0145)	0.0063^a
Superior frontal gyrus	−0.0111 (−0.0435, 0.0213)	0.4970	−0.0230 (−0.0533, 0.0073)	0.1357	−0.0151 (−0.0448, 0.0147)	0.3182
Pars opercularis	−0.0187 (−0.0557, 0.0182)	0.3171	−0.0461 (−0.0861, −0.0060)	0.0246	−0.0311 (−0.0642, 0.0020)	0.0654
Pars orbitalis	−0.0456 (−0.0984, 0.0072)	0.0899	0.0250 (−0.0229, 0.0730)	0.3029	−0.0083 (−0.0498, 0.0332)	0.6927
Pars triangularis	−0.0379 (−0.0797, 0.0040)	0.0760	−0.0770 (−0.1135, −0.0405)	0.0001^a	−0.0562 (−0.0905, −0.0220)	0.0015^a
Caudal middle frontal gyrus	−0.0453 (−0.0825, −0.0081)	0.0176	−0.0586 (−0.0982, −0.0190)	0.0042^a	−0.0509 (−0.0852, −0.0165)	0.0041^a
Rostral middle frontal gyrus	−0.0229 (−0.0544, 0.0087)	0.1536	−0.0586 (−0.0865, −0.0308)	0.0001^a	−0.0395 (−0.0665, −0.0126)	0.0045^a
Lateral orbitofrontal cortex	−0.0294 (−0.0648, 0.0061)	0.1038	−0.0177 (−0.0559, 0.0205)	0.3608	−0.0224 (−0.0554, 0.0105)	0.1793
Medial orbitofrontal cortex	−0.0337 (−0.0731, 0.0058)	0.0933	−0.0071 (−0.0499, 0.0357)	0.7422	−0.0182 (−0.0523, 0.0160)	0.2949
Occipital lobe						
Cuneus	0.0039 (−0.0262, 0.0341)	0.7968	−0.0078 (−0.0401, 0.0244)	0.6308	−0.0012 (−0.0290, 0.0267)	0.9334
Lateral occipital cortex	−0.0106 (−0.0420, 0.0209)	0.5069	0.0145 (−0.0184, 0.0474)	0.3830	0.0032 (−0.0264, 0.0328)	0.8293
Lingual gyrus	0.0173 (−0.0115, 0.0462)	0.2360	0.0140 (−0.0154, 0.0435)	0.3470	0.0189 (−0.0075, 0.0453)	0.1580
Pericalcarine	0.0029 (−0.0257, 0.0314)	0.8418	0.0131 (−0.0155, 0.0418)	0.3657	0.0082 (−0.0152, 0.0316)	0.4882
Parietal lobe						
Inferior parietal cortex	−0.0214 (−0.0541, 0.0112)	0.1957	−0.0298 (−0.0633, 0.0036)	0.0799	−0.0248 (−0.0548, 0.0052)	0.1040
Postcentral gyrus	−0.0214 (−0.0534, 0.0106)	0.1883	−0.0499 (−0.0788, −0.0210)	0.0009^a	−0.0325 (−0.0597, −0.0052)	0.0200
Precuneus	−0.0436 (−0.0744, −0.0127)	0.0061	−0.0242 (−0.0591, 0.0107)	0.1727	−0.0317 (−0.0618, −0.0016)	0.0395
Superior parietal cortex	0.0075 (−0.0269, 0.0420)	0.6657	−0.0023 (−0.0361, 0.0315)	0.8917	0.0060 (−0.0258, 0.0379)	0.7076
Supramarginal gyrus	−0.0326 (−0.0684, 0.0032)	0.0741	−0.0586 (−0.0922, −0.0250)	0.0008^a	−0.0443 (−0.0749, −0.0137)	0.0050^a
Temporal lobe						
Banks of superior temporal sulcus	−0.0547 (−0.0943, −0.0151)	0.0072^a	−0.0259 (−0.0681, 0.0162)	0.2251	−0.0394 (−0.0707, −0.0081)	0.0142^a
Inferior temporal cortex	−0.0478 (−0.0829, −0.0127)	0.0081^a	−0.0301 (−0.0653, 0.0051)	0.0930	−0.0371 (−0.0676, −0.0067)	0.0174
Middle temporal gyrus	−0.0486 (−0.0831, −0.0142)	0.0061^a	−0.0475 (−0.0818, −0.0132)	0.0071^a	−0.0473 (−0.0766, −0.0180)	0.0018^a
Superior temporal gyrus	−0.0381 (−0.0740, −0.0021)	0.0382	−0.0622 (−0.0972, −0.0271)	0.0007^a	−0.0480 (−0.0796, −0.0164)	0.0033^a
Transverse temporal gyrus	−0.0409 (−0.0955, 0.0138)	0.1409	−0.0440 (−0.1000, 0.0120)	0.1222	−0.0415 (−0.0892, 0.0062)	0.0877
Entorhinal cortex	−0.0666 (−0.1488, 0.0157)	0.1114	−0.0539 (−0.1398, 0.0321)	0.2171	−0.0601 (−0.1302, 0.0101)	0.0926
Fusiform gyrus	−0.0549 (−0.0894, −0.0205)	0.0021^a	−0.0353 (−0.0690, −0.0016)	0.0405	−0.0453 (−0.0756, −0.0150)	0.0038^a
Parahippocampal gyrus	−0.0347 (−0.1091, 0.0397)	0.3573	−0.0424 (−0.1106, 0.0258)	0.2204	−0.0360 (−0.1000, 0.0279)	0.2664
Temporal pole	−0.0516 (−0.1264, 0.0231)	0.1736	−0.0957 (−0.1668, −0.0246)	0.0088^a	−0.0663 (−0.1256, −0.0070)	0.0289

Adjusted for scanner, age, ethnicity, education, smoking, at risk for hypertension, diabetes, cholesterol, inflammation, ischemic heart disease, and the random effect of family ID. MRI measures adjusted for scanner and weighted average thickness.

Key: BMI, body mass index; CI, confidence interval; FDR, false discovery rate; MRI, magnetic resonance imaging.

^a Indicates $p < 0.05$, FDR corrected (bold values). Negative sign indicates that the region is thinner in participants who are obese (BMI ≥ 30) compared with those who are not obese (BMI < 30) at time 4 (age 62).

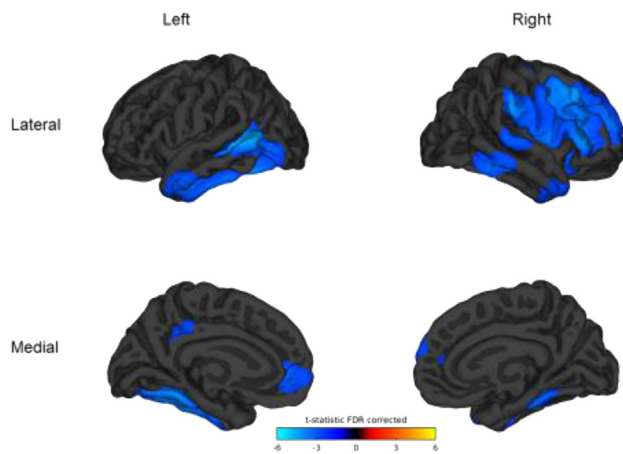


Fig. 2. Vertexwise comparisons by trajectory group. Blue color tones indicate areas in which the obesity trajectory is significantly thinner than the normal trajectory (t -test threshold > 2). Comparisons are significant at $p < 0.05$, FDR corrected. Cortical vertexwise analysis is conducted in Matlab r2014a using the Matlab FreeSurfer and Statistical toolboxes. Cortical thickness maps for each hemisphere were concatenated, and a general linear mixed model was run contrasting the BMI trajectories (different intercept, different slope) while controlling education, ethnicity, age, risk for dyslipidemia, hypertension, diabetes, ischemic heart disease, and scanner. To improve sensitivity and signal to noise ratio, a 30-mm full-wide half-maximum smoothing kernel was applied as recommended (Lerch and Evans, 2005). Significance was set at $p < 0.05$ (FDR corrected) for clusters larger than 100 voxels, and statistic maps were rendered over the FreeSurfer average brain. Abbreviations: BMI, body mass index; FDR, false discovery rate; ROI, region of interest. (For interpretation of the references to color in this figure legend, the reader is referred to the Web version of this article.)

vertexwise analyses show the obesity trajectory with significantly thinner cortex ($p < 0.05$, FDR corrected) in clusters representing the right medial superior frontal cortex, right pars opercularis, right pars triangularis, right caudal middle frontal gyri, right and left rostral middle frontal gyri, left isthmus, left rostral anterior cingulate, as well as in both right and left temporal lobes and fusiform gyri (Fig. 2; regions in blue have t -test thresholds > 2).

3.4.1. BMI trajectories and hemisphere-specific ROI cortical thickness

We then examined associations between BMI phenotypes and cortical ROIs, separately by hemisphere, using mixed models with all covariates and the random effect of twin. In the right hemisphere, the obesity trajectory compared with the normal trajectory group had a thinner cortex in the precentral gyrus, pars opercularis, pars triangularis, caudal and rostral middle frontal gyri, middle and superior temporal gyri, and temporal pole (Table 2). In the left hemisphere, the obese trajectory had significantly thinner banks of the superior temporal sulcus, inferior and middle temporal cortex, and fusiform gyrus compared with the normal trajectory. No regions in the right or left cingulate, occipital, or parietal lobes or in the left frontal lobe were significant after FDR correction.

3.4.2. Obese/nonobese groups at time 4 and hemisphere-specific ROI cortical thickness

With regard to obese/nonobese group comparisons at time 4 (Table 3), the obese group had thinner right precentral gyrus, right pars triangularis, right caudal and rostral middle frontal gyri, right postcentral gyrus, right supramarginal gyrus, right middle and superior temporal gyri, and right temporal pole, as well as left banks of superior temporal sulcus, left inferior and middle temporal cortex, and left fusiform gyrus compared with the nonobese group. Of interest in the obese/nonobese comparisons is the emergence of

significant differences in 2 right parietal ROIs (postcentral gyrus and supramarginal gyrus) that had not remained significant after FDR correction in the trajectory analyses. There were no significant associations between BMI measured continuously at age 62 and lateralized cortical thickness ROIs (data not shown).

3.5. White matter volume and abnormalities

There were no significant associations between trajectory group and total WM volume ($\beta = 0.0001$, $p = 0.98$) or abnormal WM volume ($\beta = -0.0097$, $p = 0.91$). Associations between time 4 obesity and total WM volume ($\beta = -0.0003$, $p = 0.97$) or abnormal WM volume ($\beta = -0.0200$, $p = 0.85$) were not significant (or at other timepoints, data not shown).

4. Discussion

Among men who were healthy, trajectories with steeper increases in continuously measured BMI across 4 decades were associated with having thinner cortices in late midlife, predominantly in temporal and frontal regions, despite most of these men having BMI in the normal range at the age 20 baseline. Cross-sectional results for obesity—but not continuously measured BMI—at age 62 closely paralleled those for BMI trajectory. Results for the frontal lobe appeared primarily in the right hemisphere; cortical thinness in the temporal lobe occurred in both hemispheres. Having a thinner cortex in temporal regions has most strongly predicted dementia-related outcomes in some studies. McEvoy et al. reported that temporal lobe thinning predicted more rapid onset of mild cognitive impairment and/or AD-like dementias (McEvoy et al., 2009). A study of 8 AD-related cortical regions in middle-aged adults, (Pettigrew et al., 2016) found that overall thinness in those regions predicted development of clinical AD symptoms and tau pathology across 7 years; 4 of the 7 regions overlapped our temporal lobe regions (Pettigrew et al., 2016). Comparable to a number of other studies, BMI as a continuous measure was not associated with cortical thickness. This suggests that being obese by late midlife is likely the more salient BMI phenotype related to the brain outcomes.

Longitudinal studies of BMI and cortical thickness in adults from young adulthood to late midlife are rare. In 1 other longitudinal study of adults in their 40s (Shaw et al., 2017), increasing BMI across 8 years was associated with thinning in the posterior cingulate (bilaterally), as well as thinning in the right lingual gyrus, anterior cingulate, and pericalcarine sulcus ($p < 0.05$, 1-sided) in vertexwise analyses. (Shaw et al., 2018) further reported that baseline BMI in 60- to 66-year-olds, but not 40-year-olds, was associated with cortical thickness 8 years later—most notably in the bilateral entorhinal cortex and bilateral cingulate. Increasing BMI across 8 years was associated with cortical thinning in multiple lateralized ROIs mainly in the late-life group. Our analyses only found thinner cortex in portions of the cingulate in the vertexwise analyses and in the right hemisphere of obese participants. Overall, our strongest results were in the temporal and frontal regions. It may be that the differences are due to participant characteristics such as gender (VETSA is all male, the Shaw sample was approximately 54% female), age, or study duration (42 years vs. 8 years). Nevertheless, these results suggest that the effects of excessive adiposity and associated processes on the brain likely start appearing by midlife. It is unknown if these effects are reversible; previous research found that caloric restriction improved memory performance in older adults; it is possible that reasonable reduction in BMI could have an effect on cortical thickness (Witte et al., 2009).

Although the obesity paradox—the controversial finding by some researchers that while high midlife BMI increases risk for

cognitive decline and dementia, higher late-life BMI may be protective—is often studied with regard to cognition, it is less often examined in brain phenotypes. This study finds support for an association between the role of excess BMI by late midlife and brain vulnerability. (Shaw et al., 2018) compared younger and older groups as a way of elucidating the paradox. Consistent with the paradox, increasing BMI was associated with greater cortical thinning over time (primarily in the older group); however, decreasing BMI across 8 years in the older group, but not the younger group, was also associated with greater cortical thinning in multiple ROIs. Among older adults with AD, however, (Malpetti et al., 2018) reported that having a higher BMI was associated with greater brain vulnerability for women but not men, finding no evidence that higher BMI was protective; brain vulnerability was defined as brain hypometabolism and lower metabolic connectivity in key resting-state networks. In our analyses, we found no evidence for high BMI as being protective. Given that the age range of our sample falls between those of the Shaw et al. groups, this is perhaps not unexpected and may be due to the relatively young age (average age 62) or high levels of BMI. In future studies, however, a longitudinal design combined with early measures of BMI and brain will help to elucidate the obesity paradox and how risks associated with BMI may change across the life course as well as illuminate the roles of factors such as health, age, and selective attrition, among others, in this phenomenon.

Finally, although some studies find associations between BMI and WM abnormalities, there were no significant associations in our analyses. Causes of WM abnormalities include vasculopathy, demyelination, and gliosis, but the most common cause associated with aging and cerebrovascular disease is ischemic pathogenesis or small cerebral vessel disease (Fennema-Notestine et al., 2016; Santos et al., 2017b). It may be the VETSA participants are too young (average age 62) to detect these associations. In addition, the sample had low rates of ischemic heart disease.

A number of mechanisms may link excessive midlife BMI with neurodegenerative damage; these likely are interlinked mechanisms that include vascular and metabolic pathways, inflammatory processes, and possibly genetic influences. BMI is strongly associated with poor outcomes on cardiometabolic and cardiovascular measures (Grundy, 2004; Reilly and Kelly, 2011; Reis et al., 2015; Twig et al., 2016; Xian et al., 2017). Our analyses controlled for multiple risks for cardiometabolic disease and still found significant associations between BMI trajectory and/or obesity with cortical thickness at midlife. Higher levels of BMI may also decrease cerebral blood flow and cardiac output distribution to the brain with age (Xing et al., 2017). Studies of the lipidome suggest that complex interactive processes are involved with body mass, lipid dynamics, cell metabolism, and brain morphology; lipids have essential roles in cellular signaling and membrane protein assembly, and AD progression is strongly associated with abnormal lipid metabolism (Li et al., 2017; Nam et al., 2017). Epigenetic mechanisms such as those involved in DNA methylation may also be involved; a study of the Dutch Hunger Winter, for example, found that epigenetic factors mediated associations between exposure to adversity during early development and BMI in adulthood (Tobi et al., 2018). Such risk factors are also likely to play a role in brain development. Explorations of the substantial genetic overlap between cardiometabolic indicators, inflammation, and BMI may also yield further insights into the biology of obesity, neurodegenerative damage, and comorbidity with other disease processes (Locke et al., 2015; Marioni et al., 2016; Panizzon et al., 2015; Santos et al., 2017a). For instance, in a genome-wide association study meta-analysis, the most strongly enriched gene sets for BMI and obesity involved critical brain pathways regulating appetite, insulin synthesis and processing, and energy metabolism in the hypothalamus

and pituitary, synaptic plasticity, and cellular mechanisms (Locke et al., 2015). Genetic analyses were beyond the scope of this study.

Our study has several limitations. Longitudinal MRI data were not available so we were unable to evaluate whether the brain structures were different at earlier time periods. Scanner selection criteria typically exclude extremely heavy men (i.e., girth greater than the MRI bore and/or, in these scanners, weight greater than 300 pounds), which restricts examination of brain phenotypes in more extreme cases. Studies focused on older adults, however, likely already have high levels of selective attrition associated with obesity related to both health and scanner limitations. Waist circumference is sometimes considered a better indicator of adiposity than BMI (Connor-Gorber et al., 2007), but BMI was our only measure with multiple timepoints, which allowed for trajectory and longitudinal analyses. Moreover, BMI and waist circumference in the present sample were correlated $r = 0.90$. BMI data at time 2 were self-reported; misestimation of self-reported BMI has been shown in different groups (Richmond et al., 2015). The sample is primarily male non-Hispanic white veterans, so generalizability to women and other groups is unclear. Recent longitudinal studies find some sex differences in associations with BMI (von Bonsdorff et al., 2015). A strength of the study includes the homogeneity of age in an all-male sample, thereby increasing our power.

5. Conclusions

To our knowledge, this study is unique in its analyses of 4 decades of longitudinal BMI data starting in young adulthood and the relationship of BMI phenotypes with cortical thickness and WM in late midlife. This large age-homogeneous sample allowed for in-depth examination of BMI change and heterogeneity across an important transitional age period when cardiometabolic dysregulation and inflammation become more prevalent (Locke et al., 2015). We provided evidence that either steeply increasing BMI from young adulthood to late midlife or obesity in late midlife is significantly associated with thinner cortex in late midlife, predominantly in the frontal and temporal lobes. Results for the BMI trajectory and time 4 obesity analyses were comparable, so there appears to be no statistical advantage to examining trajectories over current obesity. In contrast to the BMI trajectories, however, continuously measured BMI at time 4 was not associated with cortical thickness. Knowing what trajectory a person is on earlier in adulthood may also be clinically useful (Croswell and Luger, 2012). Taken in the context of other research, these associations with excess BMI at midlife portend potentially increased risk for cognitive decline (Albanese et al., 2017; Chuang et al., 2016) and reduced life expectancy in later life (Olshansky et al., 2005).

Disclosure

AMD is a founder of and holds equity in CorTechs Laboratories, Inc, and serves on its Scientific Advisory Board. He is a member of the Scientific Advisory Board of Human Longevity, Inc, and receives funding through research agreements with General Electric Healthcare and Medtronic, Inc. The terms of these arrangements have been reviewed and approved by the University of California, San Diego in accordance with its conflict of interest policies. Other authors report no financial interests.

Acknowledgements

The U.S. Department of Veterans Affairs, Department of Defense; National Personnel Records Center, National Archives and Records Administration; Internal Revenue Service; National Opinion Research Center; National Research Council, National Academy of

Sciences; and the Institute for Survey Research, Temple University provided invaluable assistance in the conduct of the VET Registry. The authors gratefully acknowledge the continued cooperation of the twins and the efforts of many staff members.

This work was supported by the National Institutes of Health, National Institute on Aging, grants number R01s AG050595, AG022381-15, and R01 AG059329. AB was also supported by R25 AG043364. Content of this manuscript is the responsibility of the authors and does not represent official views of NIH or the Veterans' Administration. The funding sources had no involvement in study design or collection, analysis, or interpretation of data, the writing of the report, or decision to submit the article for publication.

Appendix A. Supplementary data

Supplementary data associated with this article can be found, in the online version, at <https://doi.org/10.1016/j.neurobiolaging.2019.03.003>.

References

- Albanese, E., Launer, L.J., Egger, M., Prince, M.J., Giannakopoulos, P., Wolters, F.J., Egan, K., 2017. Body mass index in midlife and dementia: systematic review and meta-regression analysis of 589,649 men and women followed in longitudinal studies. *Alzheimers Dement. (Amst.)* 8, 165–178.
- Aronow, W.S., Fleg, J.L., Pepine, C.J., Artinian, N.T., Bakris, G., Brown, A.S., Ferdinand, K.C., Forciea, M.A., Frishman, W.H., Jaigobin, C., Kostis, J.B., Mancina, G., Oparil, S., Ortiz, E., Reisin, E., Rich, M.W., Schocken, D.D., Weber, M.A., Wesley, D.J., Harrington, R.A., 2011. ACCF/AHA 2011 expert consensus document on hypertension in the elderly: a report of the American college of cardiology foundation task force on clinical expert consensus documents. *Circulation* 123, 2434–2506.
- Benjamini, Y., Hochberg, Y., 1995. Controlling the false discovery rate: a practical and powerful approach to multiple testing. *J. R. Stat. Soc. Ser. B Stat Methodol* 57, 289–300.
- Bernal-Rusiel, J.L., Atienza, M., Cantero, J.L., 2010. Determining the optimal level of smoothing in cortical thickness analysis: a hierarchical approach based on sequential statistical thresholding. *Neuroimage* 52, 158–171.
- Cawley, J., Maclean, J.C., 2012. Unfit for Service: the implications of rising obesity for U.S. Military recruitment. *Health Econ.* 21, 1348–1366.
- Chuang, Y.F., An, Y., Bilgel, M., Wong, D.F., Troncoso, J.C., O'Brien, R.J., Breitner, J.C., Ferrucci, L., Resnick, S.M., Thambisetty, M., 2016. Midlife adiposity predicts earlier onset of Alzheimer's dementia, neuropathology and presymptomatic cerebral amyloid accumulation. *Mol. Psychiatry* 21, 910–915.
- Connor-Gorber, S., Tremblay, A., Moher, D., Gorber, B., 2007. A comparison of direct vs. self-report measures for assessing height, weight and body mass index: a systematic review. *Obes. Rev.* 8, 307–326.
- Coutinho, A.M., Couto, J.P., Lindemer, E.R., Rosas, H.D., Rosen, B.R., Salat, D.H., 2017. Differential associations between systemic markers of disease and cortical thickness in healthy middle-aged and older adults. *Neuroimage* 146, 19–27.
- Crosswell, J., Luger, S., 2012. Screening for and management of obesity in adults. *Am. Fam. Physician* 86, 947–948.
- Desikan, R.S., Segonne, F., Fischl, B., Quinn, B.T., Dickerson, B.C., Blacker, D., Buckner, R.L., Dale, A.M., Maguire, R.P., Hyman, B.T., Albert, M.S., Killiany, R.J., 2006. An automated labeling system for subdividing the human cerebral cortex on MRI scans into gyral based regions of interest. *Neuroimage* 31, 968–980.
- Fennema-Notestine, C., McEvoy, L.K., Notestine, R., Panizzon, M.S., Yau, W.W., Franz, C.E., Lyons, M.J., Eyler, L.T., Neale, M.C., Xian, H., McKenzie, R.E., Kremen, W.S., 2016. White matter disease in midlife is heritable, related to hypertension, and shares some genetic influence with systolic blood pressure. *Neuroimage Clin.* 12, 737–745.
- Fischl, B., 2012. Freesurfer. *Neuroimage* 62, 774–781.
- Fjell, A.M., Westlye, L.T., Grydeland, H., Amlien, I., Espeseth, T., Reinvang, I., Raz, N., Dale, A.M., Walhovd, K.B., Alzheimer Disease Neuroimaging Initiative, 2014. Accelerating cortical thinning: unique to dementia or universal in aging? *Cereb. Cortex* 24, 919–934.
- Goldberg, J., Curran, B., Vitek, M.E., Henderson, W.G., Boyko, E.J., 2002. The Vietnam Era twin registry. *Twin Res.* 5, 476–481.
- Grundey, S.M., 2004. Obesity, metabolic syndrome, and cardiovascular disease. *J. Clin. Endocrinol. Metab.* 89, 2595–2600.
- Jovicich, J., Czanner, S., Greve, D., Haley, E., van der Kouwe, A., Gollub, R., Kennedy, D., Schmitt, F., Brown, G., Macfall, J., Fischl, B., Dale, A.M., 2006. Reliability in multi-site structural MRI studies: effects of gradient non-linearity correction on phantom and human data. *Neuroimage* 30, 436–443.
- Kremen, W.S., Fennema-Notestine, C., Eyler, L.T., Panizzon, M.S., Chen, C.H., Franz, C.E., Lyons, M.J., Thompson, W.K., Dale, A.M., 2013a. Genetics of brain structure: contributions from the Vietnam Era twin study of aging. *Am. J. Med. Genet. B Neuropsychiatr. Genet.* 162B, 751–761.
- Kremen, W.S., Franz, C.E., Lyons, M.J., 2013b. VETSA: the Vietnam Era twin study of aging. *Twin Res. Hum. Genet.* 16, 399–402.
- Kremen, W.S., Thompson-Brenner, H., Leung, Y.M., Grant, M.D., Franz, C.E., Eisen, S.A., Jacobson, K.C., Boake, C., Lyons, M.J., 2006. Genes, environment, and time: the Vietnam Era twin study of aging (VETSA). *Twin Res. Hum. Genet.* 9, 1009–1022.
- Krishnadas, R., McLean, J., Batty, G.D., Burns, H., Deans, K.A., Ford, I., McConnachie, A., McGinty, A., McLean, J.S., Millar, K., Sattar, N., Shiels, P.G., Velupillai, Y.N., Packard, C.J., Cavanagh, J., 2013. Cardio-metabolic risk factors and cortical thickness in a neurologically healthy male population: results from the psychological, social and biological determinants of ill health (pSoBid) study. *Neuroimage Clin.* 2, 646–657.
- Lampe, F.C., Walker, M., Lennon, L.T., Whincup, P.H., Ebrahim, S., 1999. Validity of a self-reported history of doctor-diagnosed angina. *J. Clin. Epidemiol.* 52, 73–81.
- Lerch, J.P., Evans, A.C., 2005. Cortical thickness analysis examined through power analysis and a population simulation. *Neuroimage* 24, 163–173.
- Li, J., Ji, L., 2005. Adjusting multiple testing in multilocus analyses using the eigenvalues of a correlation matrix. *Heredity (Edinb)* 95, 221–227.
- Li, Q., Bozek, K., Xu, C., Guo, Y., Sun, J., Paabo, S., Sherwood, C.C., Hof, P.R., Ely, J.J., Li, Y., Willmitzer, L., Giallisco, P., Khaitovich, P., 2017. Changes in lipidome composition during brain development in humans, chimpanzees, and macaque monkeys. *Mol. Biol. Evol.* 34, 1155–1166.
- Locke, A.E., Kahali, B., Berndt, S.I., Justice, A.E., Pers, T.H., Day, F.R., Powell, C., Vedantam, S., Buchkovich, M.L., Yang, J., Croteau-Chonka, D.C., Esko, T., Fall, T., Ferreira, T., Gustafsson, S., Kutalik, Z., Luan, J., Magi, R., Randall, J.C., Winkler, T.W., Wood, A.R., Workalemahu, T., Faul, J.D., Smith, J.A., Hu, Zhao, J., Zhao, W., Chen, J., Fehrmann, R., Hedman, A.K., Karjalainen, J., Schmidt, E.M., Absher, D., Amin, N., Anderson, D., Beekman, M., Bolton, J.L., Bragg-Gresham, J.L., Buyske, S., Demirkan, A., Deng, G., Ehret, G.B., Feenstra, B., Feitosa, M.F., Fischer, K., Goel, A., Gong, J., Jackson, A.U., Kanoni, S., Kleber, M.E., Kristiansson, K., Lim, U., Lotay, V., Mangino, M., Mateo Leach, I., Medina-Gomez, C., Medland, S.E., Nalls, M.A., Palmer, C.D., Pasko, D., Pechlivanis, S., Peters, M.J., Prokopenko, I., Shungin, D., Stancakova, A., Strawbridge, R.J., Ju Sung, Y., Tanaka, T., Teumer, A., Trompet, S., van der Laan, S.W., van Setten, J., Van Vliet-Ostaptchouk, J.V., Wang, Z., Yengo, L., Zhang, W., Isaacs, A., Albrecht, E., Arnlöv, J., Arscott, G.M., Attwood, A.P., Bandinelli, S., Barrett, A., Bas, I.N., Bellis, C., Bennett, A.J., Berne, C., Blagieva, R., Blüher, M., Bohringer, S., Bonnycastle, L.L., Bottcher, Y., Boyd, H.A., Bruinenberg, M., Caspersen, I.H., Ida Chen, Y.D., Clarke, R., Daw, E.W., de Craen, A.J., Delgado, G., Dimitriou, M., Doney, A.S., Eklund, N., Estrada, K., Eury, E., Folkersen, L., Fraser, R.M., Garcia, M.E., Geller, F., Giedraitis, V., Gigante, B., Go, A.S., Golay, A., Goodall, A.H., Gordon, S.D., Gorski, M., Grabe, H.J., Grallert, H., Grammer, T.B., Grassler, J., Gronberg, H., Groves, C.J., Gusto, G., Haessler, J., Hall, P., Haller, T., Hallmans, G., Hartman, C.A., Hassinen, M., Hayward, C., Heard-Costa, N.L., Helmer, Q., Hengstenberg, C., Holmen, O., Hottenga, J.J., James, A.L., Jeff, J.M., Johansson, A., Jolley, J., Juliusdottir, T., Kinnunen, L., Koenig, W., Koskenvuo, M., Kratzer, W., Laitinen, J., Lamina, C., Leander, K., Lee, N.R., Lichtner, P., Lind, L., Lindstrom, J., Sin Lo, K., Lobbens, S., Lohrbe, R., Lu, Y., Mach, F., Magnusson, P.K., Mahajan, A., McArdle, W.L., McLachlan, S., Menni, C., Merger, S., Mihailov, E., Milani, L., Moayyeri, A., Monda, K.L., Morken, M.A., Mullas, A., Muller, G., Muller-Nurasyid, M., Musk, A.W., Nagaraja, R., Nothen, M.M., Nolte, I.M., Pilz, S., Rayner, N.W., Renstrom, F., Rettig, R., Ried, J.S., Ripke, S., Robertson, N.R., Rose, L.M., Sanna, S., Scharnagl, H., Scholtens, S., Schumacher, F.R., Scott, W.R., Seufferlein, T., Shi, J., Vernon Smith, A., Smolonska, J., Stanton, A.V., Steinthorsdottir, V., Stirrups, K., Stringham, H.M., Sundstrom, J., Swertz, M.A., Swift, A.J., Syvanen, A.C., Tan, S.T., Tayo, B.O., Thorand, B., Thorleifsson, G., Tyrer, J.P., Uhl, H.W., Vandenput, L., Verhulst, F.C., Vermeulen, S.H., Verweij, N., Vonk, J.M., Waite, L.L., Warren, H.R., Waterworth, D., Weedon, M.N., Wilkens, L.R., Willenborg, C., Wilsgaard, T., Wojczynski, M.K., Wong, A., Wright, A.F., Zhang, Q., Brennan, E.P., Choi, M., Dastani, Z., Drong, A.W., Eriksson, P., Franco-Cereceda, A., Gadin, J.R., Gharavi, A.G., Goddard, M.E., Handsaker, R.E., Huang, J., Karpe, F., Kathiresan, S., Keildson, S., Kiryluk, K., Kubo, M., Lee, J.Y., Liang, L., Lifton, R.P., Ma, B., McCarroll, S.A., McKnight, A.J., Min, J.L., Moffatt, M.F., Montgomery, G.W., Murabito, J.M., Nicholson, G., Nyholt, D.R., Okada, Y., Perry, J.R., Dorajoo, R., Reinmaa, E., Salem, R.M., Sandholm, N., Scott, R.A., Stolk, L., Takahashi, A., Van't Hooft, F.M., Vinkhuysen, A.A., Westra, H.J., Zheng, W., Zondervan, K.T., ADIPOGen Consortium; AGES-BMI Working Group; CARDIOGRAMplusC4D Consortium; CKDGen Consortium; GLGC; ICBP; MAGIC Investigators; MuTHER Consortium; MIGen Consortium; PAGE Consortium; ReproGen Consortium; GENIE Consortium; International Endogene Consortium; Heath A.C., Arveiler, D., Bakker, S.J., Beilby, J., Bergman, R.N., Blangero, J., Bovet, P., Campbell, H., Caulfield, M.J., Cesana, G., Chakravarti, A., Chasman, D.I., Chines, P.S., Collins, F.S., Crawford, D.C., Cupples, L.A., Cusi, D., Danesh, J., de Faire, U., den Ruijter, H.M., Dominiczak, A.F., Erbel, R., Erdmann, J., Eriksson, J.G., Farrall, M., Felix, S.B., Ferrannini, E., Ferrieres, J., Ford, I., Forouhi, N.G., Forrester, T., Franco, O.H., Gansevoort, R.T., Gejman, P.V., Gieger, C., Gottesman, O., Gudnason, V., Gyllenstein, U., Hall, A.S., Harris, T.B., Hattersley, A.T., Hicks, A.A., Hindorf, L.A., Hingorani, A.D., Hofman, A., Homuth, G., Hovingh, G.K., Humphries, S.E., Hunt, S.C., Hyppönen, E., Illig, T., Jacobs, K.B., Jarvelin, M.R., Jockel, K.H., Johansen, B., Jousilahti, P., Jukema, J.W., Julia, A.M., Kaprio, J., Kastelein, J.J., Keinanen-Kiukkaanniemi, S.M., Kiemeny, L.A., Knekt, P., Kooner, J.S., Kooperberg, C., Kovacs, P., Kraja, A.T., Kumari, M., Kuusisto, J., Lakka, T.A., Langenberg, C., Le Marchand, L., Lehtimäki, T., Lysenko, V., Mannisto, S., Marette, A., Matise, T.C., McKenzie, C.A., McKnight, B., Moll, F.L., Morris, A.D.,

- Morris, A.P., Murray, J.C., Nelis, M., Ohlsson, C., Oldehinkel, A.J., Ong, K.K., Madden, P.A., Pasterkamp, G., Peden, J.F., Peters, A., Postma, D.S., Pramstaller, P.P., Price, J.F., Qi, L., Raitakari, O.T., Rankinen, T., Rao, D.C., Rice, T.K., Ridker, P.M., Rioux, J.D., Ritchie, M.D., Rudan, I., Salomaa, V., Samani, N.J., Saramies, J., Sarzynski, M.A., Schunkert, H., Schwarz, P.E., Sever, P., Shuldiner, A.R., Sinisalo, J., Stolk, R.P., Strauch, K., Tonjes, A., Tregouet, D.A., Tremblay, A., Tremoli, E., Virtamo, J., Vohl, M.C., Volker, U., Waeber, G., Willemssen, G., Witteman, J.C., Zillikens, M.C., Adair, L.S., Amouyel, P., Asselbergs, F.W., Assimes, T.L., Bochud, M., Boehm, B.O., Boerwinkle, E., Bornstein, S.R., Bottinger, E.P., Bouchard, C., Cauchi, S., Chambers, J.C., Chanoock, S.J., Cooper, R.S., de Bakker, P.I., Dedoussis, G., Ferrucci, L., Franks, P.W., Froguel, P., Groop, L.C., Haiman, C.A., Hamsten, A., Hui, J., Hunter, D.J., Hveem, K., Kaplan, R.C., Kivimaki, M., Kuh, D., Laakso, M., Liu, Y., Martin, D.G., Marz, W., Melbye, M., Metspalu, A., Moebus, S., Munroe, P.B., Njolstad, I., Oostra, B.A., Palmer, C.N., Pedersen, N.L., Perola, M., Perusse, L., Peters, U., Power, C., Quertermous, T., Rauramaa, R., Rivadeneira, F., Saaristo, T.E., Saleheen, D., Sattar, N., Schadt, E.E., Schlessinger, D., Slagboom, P.E., Snieder, H., Spector, T.D., Thorsteinsdottir, U., Stumvoll, M., Tuomilehto, J., Uitterlinden, A.G., Uusitupa, M., van der Harst, P., Walker, M., Wallaschofski, H., Wareham, N.J., Watkins, H., Weir, D.R., Wichmann, H.E., Wilson, J.F., Zanen, P., Borecki, I.B., Deloukas, J., Fox, C.S., Heid, I.M., O'Connell, J.R., Strachan, D.P., Stefansson, K., van Duijn, C.M., Abecasis, G.R., Franke, L., Frayling, T.M., McCarthy, M.I., Visscher, P.M., Schrag, A., Willer, C.J., Boehnke, M., Mohlke, K.L., Lindgren, C.M., Beckmann, J.S., Barrois, I., North, K.E., Ingelsson, E., Hirschhorn, J.N., Loos, R.J., Speliotes, E.K., 2015. Genetic studies of body mass index yield new insights for obesity biology. *Nature* 518, 197–206.
- Malpetti, M., Sala, A., Vanoli, E.G., Gianolli, L., Luzzi, L., Perani, D., 2018. Unfavourable gender effect of high body mass index on brain metabolism and connectivity. *Sci. Rep.* 8, 12584.
- Marioni, R.E., Yang, J., Dykiert, D., Mottus, R., Campbell, A., Davies, G., Hayward, C., Porteous, D.J., Visscher, P.M., Deary, I.J., 2016. Assessing the genetic overlap between BMI and cognitive function. *Mol. Psychiatry* 21, 1477–1482.
- McEvoy, L.K., Fennema-Notestine, C., Roddey, J.C., Hagler Jr., D.J., Holland, D., Karow, D.S., Pung, C.J., Brewer, J.B., Dale, A.M., Alzheimer's Disease Neuroimaging Initiative, 2009. Alzheimer disease: quantitative structural neuroimaging for detection and prediction of clinical and structural changes in mild cognitive impairment. *Radiology* 251, 195–205.
- Medic, N., Ziauddeen, H., Ersche, K.D., Farooqi, I.S., Bullmore, E.T., Nathan, P.J., Ronan, L., Fletcher, P.C., 2016. Increased body mass index is associated with specific regional alterations in brain structure. *Int. J. Obes. (Lond)* 40, 1177–1182.
- Mora, S., Musunuru, K., Blumenthal, R.S., 2009. The clinical utility of high-sensitivity C-reactive protein in cardiovascular disease and the potential implication of JUPITER on current practice guidelines. *Clin. Chem.* 55, 219–228.
- Muthén, L.K., Muthén, B.O., 2015. *Mplus User's Guide*, 7 ed. Muthén & Muthén, Los Angeles, CA.
- Nam, K.N., Mounier, A., Wolfe, C.M., Fitz, N.F., Carter, A.Y., Castranio, E.L., Kamboh, H.I., Reeves, V.L., Wang, J., Han, X., Schug, J., Lefterov, I., Koldamova, R., 2017. Effect of high fat diet on phenotype, brain transcriptome and lipidome in Alzheimer's model mice. *Sci. Rep.* 7, 4307.
- Olshansky, S.J., Passaro, D.J., Hershow, R.C., Layden, J., Carnes, B.A., Brody, J., Hayflick, L., Butler, R.N., Allison, D.B., Ludwig, D.S., 2005. A potential decline in life expectancy in the United States in the 21st century. *N. Engl. J. Med.* 352, 1138–1145.
- Panizzon, M.S., Fennema-Notestine, C., Eyler, L.T., Jernigan, T.L., Prom-Wormley, E., Neale, M., Jacobson, K., Lyons, M.J., Grant, M.D., Franz, C.E., Xian, H., Tsuang, M., Fischl, B., Seidman, L., Dale, A., Kremen, W.S., 2009. Distinct genetic influences on cortical surface area and cortical thickness. *Cereb. Cortex* 19, 2728–2735.
- Panizzon, M.S., Hauger, R.L., Sailors, M., Lyons, M.J., Jacobson, K.C., Murray McKenzie, R., Rana, B., Vasilopoulos, T., Vuoksimaa, E., Xian, H., Kremen, W.S., Franz, C.E., 2015. A new look at the genetic and environmental coherence of metabolic syndrome components. *Obesity (Silver Spring)* 23, 2499–2507.
- Pettigrew, C., Soldan, A., Zhu, Y., Wang, M.C., Moghekar, A., Brown, T., Miller, M., Albert, M., BIOCARD Research Team, 2016. Cortical thickness in relation to clinical symptom onset in preclinical AD. *Neuroimage Clin.* 12, 116–122.
- Reilly, J.J., Kelly, J., 2011. Long-term impact of overweight and obesity in childhood and adolescence on morbidity and premature mortality in adulthood: systematic review. *Int. J. Obes. (Lond)* 35, 891–898.
- Reis, J.P., Allen, N., Gunderson, E.P., Lee, J.M., Lewis, C.E., Loria, C.M., Powell-Wiley, T.M., Rana, J.S., Sidney, S., Wei, G., 2015. Excess body mass index and waist circumference-years and incident cardiovascular disease: the CARDIA study. *Obesity (Silver Spring)* 23, 879–885.
- Richmond, T.K., Thurston, I., Sonnevile, K., Milliren, C.E., Walls, C.E., Austin, S.B., 2015. Racial/ethnic differences in accuracy of body mass index reporting in a diverse cohort of young adults. *Int. J. Obes. (Lond)* 39, 546–548.
- Santos, C.Y., Snyder, P.J., Wu, W.C., Zhang, M., Echeverria, A., Alber, J., 2017a. Pathophysiological relationship between Alzheimer's disease, cerebrovascular disease, and cardiovascular risk: a review and synthesis. *Alzheimers Dement (Amst)* 7, 69–87.
- Santos, P.P., Silveira, P.S., Souza-Duran, F.L., Tamashiro-Duran, J.H., Scazufca, M., Menezes, P.R., Leite, C.D., Lotufo, P.A., Vallada, H., Wajngarten, M., De Toledo Ferraz Alves, T.C., Rzezak, P., Busatto, G.F., 2017b. Prefrontal-parietal white matter volumes in healthy elderly are decreased in proportion to the degree of cardiovascular risk and related to inhibitory control deficits. *Front. Psychol.* 8, 57.
- Schoenborn, C.A., Heyman, K.M., 2009. Health characteristics of adults aged 55 years and over: United States, 2004–2007. In: U.S. Department of Health and Human Services Centers for Disease Control and Prevention. Hyattsville, MD.
- Shaw, M.E., Abhayaratna, W.P., Anstey, K.J., Cherbuin, N., 2017. Increasing body mass index at midlife is associated with increased cortical thinning in Alzheimer's disease-vulnerable regions. *J. Alzheimers Dis.* 59, 113–120.
- Shaw, M.E., Sachdev, P.S., Abhayaratna, W., Anstey, K.J., Cherbuin, N., 2018. Body mass index is associated with cortical thinning with different patterns in mid- and late-life. *Int. J. Obes. (Lond)* 42, 455–461.
- Singh-Manoux, A., Dugravot, A., Shipley, M., Brunner, E.J., Elbaz, A., Sabia, S., Kivimaki, M., 2018. Obesity trajectories and risk of dementia: 28 years of follow-up in the Whitehall II Study. *Alzheimers Dement.* 14, 178–186.
- Sled, J.G., Zijdenbos, A.P., Evans, A.C., 1998. A nonparametric method for automatic correction of intensity nonuniformity in MRI data. *IEEE Trans. Med. Imaging* 17, 87–97.
- Tobi, E.W., Slieker, R.C., Luijk, R., Dekkers, K.F., Stein, A.D., Xu, K.M., Biobank-based Integrative Omics Studies Consortium, Slagboom, P.E., van Zwet, E.W., Lumey, L.H., Heijmans, B.T., 2018. DNA methylation as a mediator of the association between prenatal adversity and risk factors for metabolic disease in adulthood. *Sci. Adv.* 4, eaao4364.
- Twigg, G., Yaniv, G., Levine, H., Leiba, A., Goldberger, N., Derazne, E., Ben-Ami Shor, D., Tzur, D., Afek, A., Shamiss, A., Haklai, Z., Kark, J.D., 2016. Body-mass index in 2.3 million adolescents and cardiovascular death in adulthood. *N. Engl. J. Med.* 374, 2430–2440.
- von Bonsdorff, M.B., Tormakangas, T., Rantanen, T., Salonen, M.K., Osmond, C., Kajantie, E., Eriksson, J.G., 2015. Early life body mass trajectories and mortality in older age: findings from the Helsinki Birth Cohort Study. *Ann. Med.* 47, 34–39.
- Vuoksimaa, E., Panizzon, M.S., Chen, C.H., Fiecas, M., Eyler, L.T., Fennema-Notestine, C., Hagler, D.J., Fischl, B., Franz, C.E., Jak, A., Lyons, M.J., Neale, M.C., Rinker, D.A., Thompson, W.K., Tsuang, M.T., Dale, A.M., Kremen, W.S., 2015. The genetic association between neocortical volume and general cognitive ability is driven by global surface area rather than thickness. *Cereb. Cortex* 25, 2127–2137.
- Walhovd, K.B., Storsve, A.B., Westlye, L.T., Drevon, C.A., Fjell, A.M., 2014. Blood markers of fatty acids and vitamin D, cardiovascular measures, body mass index, and physical activity relate to longitudinal cortical thinning in normal aging. *Neurobiol. Aging* 35, 1055–1064.
- Willette, A.A., Kapogiannis, D., 2015. Does the brain shrink as the waist expands? *Ageing Res. Rev.* 20, 86–97.
- Witte, A.V., Fobker, M., Gellner, R., Knecht, S., Floel, A., 2009. Caloric restriction improves memory in elderly humans. *Proc. Natl. Acad. Sci. U. S. A.* 106, 1255–1260.
- Xian, H., Scherrer, J.F., Franz, C.E., McCaffery, J., Stein, P.K., Lyons, M.J., Jacobsen, K., Eisen, S.A., Kremen, W.S., 2010. Genetic vulnerability and phenotypic expression of depression and risk for ischemic heart disease in the Vietnam era twin study of aging. *Psychosom. Med.* 72, 370–375.
- Xian, H., Vasilopoulos, T., Liu, W., Hauger, R.L., Jacobson, K.C., Lyons, M.J., Panizzon, M., Reynolds, C.A., Vuoksimaa, E., Kremen, W.S., Franz, C.E., 2017. Steeper change in body mass across four decades predicts poorer cardiometabolic outcomes at midlife. *Obesity (Silver Spring)* 25, 773–780.
- Xing, C.Y., Tarumi, T., Liu, J., Zhang, Y., Turner, M., Riley, J., Tinajero, C.D., Yuan, L.J., Zhang, R., 2017. Distribution of cardiac output to the brain across the adult lifespan. *J. Cereb. Blood Flow Metab.* 37, 2848–2856.